Machine-learning prediction of facet-dependent CO coverage on Cu electrocatalysts

Shanglin Wu[1], Shisheng Zheng[2]*, Wentao Zhang[1], Mingzheng Zhang[1], Shunning Li[1]* and Feng Pan[1]*

[1] School of Advanced Materials, Peking University, Shenzhen Graduate School, Shenzhen 518055, China.

[2] College of Energy, Xiamen University, Xiamen 361000, China

*E-mail: zhengss@pku.edu.cn (S.Z.); lisn@pku.edu.cn (S.L.); panfeng@pkusz.edu.cn (F.P.)

Abstract

Copper-based electrocatalysts, which hold great promise in selectively reducing CO_2 into multicarbon products, have attracted a lot of recent interest, both experimentally and theoretically. While many studies have suggested a strong dependence of catalytic selectivity on the concentration of the *CO reaction intermediate on Cu surface, it remains challenging for a direct experimental probe of the CO coverage. This necessitates a reliable computational method that can accurately establish the theoretical coverage-dependent phase diagram of CO adsorbates on the catalyst. Here we propose a scheme composed of density functional theory (DFT) calculations, machine-learning force fields (MLFF) and graph neural networks (GNN) as a solution. This method enables a fast screening of 7 million adsorption configurations based on a small set of DFT data, with a balance between accuracy and efficiency tuned by the combinatorial use of MLFF and GNN models. We have investigated 8 different Cu facets, and discovered that the high-index facets such as (310), (210) and (322) exhibit a much higher CO coverage than the low-index counterparts such as (111), leading to an increased opportunity for C-C coupling for the former. Our results can provide a new perspective for the understanding of the fundamental role of CO coverage on Cu surface for electrochemical CO_2 reduction.

Introduction

In the realms of surface science and catalysis, the interactions between surfaces and adsorbates are foundational for understanding catalytic processes and crucial for catalyst design and discovery.[1-6] With the rapid advancement of computational and theoretical chemistry, particularly the extensive application of Density Functional Theory (DFT), researchers can now calculate the adsorption energy of adsorbates on surfaces with unprecedented accuracy, playing an indispensable role in catalyzing the design and innovation process.[6-12]

The study of lateral interactions among adsorbates and their impact on catalytic activity, selectivity, and surface stability, such as in CO_2RR, NORR, COOR, and the Fischer-Tropsch synthesis, has gained increasing attention.[13-36] These interactions, especially those modulated by varying adsorbate coverage, are vital for precisely controlling the catalytic reaction process, making a deep understanding of lateral adsorbate interactions and coverage effects crucial for optimizing catalyst design and enhancing performance. However, exhaustively calculating coverage-dependent adsorption energies using DFT alone often proves impractical due to the combinatorial growth of adsorption configuration spaces with coverage and site types, and the substantial computational cost of a comprehensive analysis. Various methods have been proposed to address this, including cluster expansion, multi-order lateral interaction models, graph theory, and machine learning approaches.[5, 35-51] The combination of graph theory and machine learning has been regarded as one of the most effective means to analyze coverage-dependent adsorption energies: graph theory tools for automating the enumeration of vast adsorption configurations, and machine learning models for predicting adsorption energies across the entire configuration space based on a limited DFT dataset.[44, 47-48, 52] However, graph-based enumeration algorithms encounter significant computational bottlenecks at the stage of isomorphism comparison of configurations, as graph isomorphism comparison is an extremely time-consuming NP problem, exponentially growing with the number of atoms in adsorption configurations.[53-54] Since the differences between adsorption configurations mainly depend on the occupation of different adsorbate sites, symmetry-based methods often offer a more efficient evaluation of adsorption configurations with multiple site occupations. Machine learning approaches, especially deep learning methods based on neural networks, have been primarily divided into two strategies for accelerating the prediction of adsorption energies in vast configuration spaces: (1) direct prediction of stable state adsorption energies from initial configuration guesses using neural networks (NNs), and (2) acceleration of the geometry optimization process using machine learning potentials (MLPs).[35-36, 47-48, 52] While neural network methods are highly efficient in prediction with negligible computational cost, their accuracy depends not only on the model quality but also on the size of the training dataset.[55] In contrast, MLP methods require significantly less DFT computational data for training and can obtain both stable configurations and more accurate adsorption energy predictions. However, the optimization time needed for MLP methods far exceeds the prediction time of NN methods, though it still represents a substantial saving in computational cost compared to direct DFT calculations. Each strategy has its strengths, and they contribute from different perspectives to the exploration of coverage-dependent adsorption energies. Yet, all these methods can only consider the optimization of a limited number of configurations, facing

insurmountable computational burdens when confronted with potentially hundreds of thousands or millions of configurations.

In this work, we have developed a "structure enumeration + MLP + NNs" approach for efficiently exploring adsorbate-adsorbate interactions, enabling the rapid exploration of nearly ten million configurations. By rapidly enumerating and deduplicating adsorption configurations through a "geometry + graph theory + symmetry" approach, we generated an approximately 7 million configuration guess space. Then, using a designated sampling method, we selected a very small set of configurations (~1592) for DFT structural optimization to obtain optimization trajectories for training a machine learning force field (MLFF) based on Deep Potential Molecular Dynamics (DPMD). Subsequently, the MLFF was used to perform structural optimizations on an expanded sampling space (~186,000) to obtain corresponding stable adsorption energies. Finally, we trained a graph embedding network model (GEN) using the configuration-energy data, which considered non-bonded adsorbate interactions in feature construction and efficiently predicted energies across the entire target configuration space. Applied to the Cu-CO system, our method achieved results qualitatively consistent with experiments at 3 orders of magnitude lower computational cost than pure DFT calculations: the adsorption strength of CO on Cu surfaces exhibited a minimal change in energy at first, followed by a significant increase with coverage; high-index Cu surfaces often exhibited higher catalytic activity due to more low-coordination Cu sites. These findings undoubtedly demonstrate the effectiveness and efficiency of our method and its power in exploring vast configuration spaces.

Results and Discussion

At high coverage, the configurations of adsorption not only experience an explosive increase in number due to the enumerated surfaces and the geometric structures and binding modes of the adsorbates but also become almost unpredictable due to the complex interactions between the adsorbates. This signifies that the enumeration methods relying solely on expert experience fail under these circumstances.[42] By integrating expert knowledge with deep learning technologies, a programmable scalable agent model can provide interpretable and reliable analysis and predictions for the vast configuration space.

Workflow

Our study focuses on the adsorption configurations of CO on eight different Cu surfaces at varying coverage levels. As illustrated in Figure 1a, taking the 100 surface as an example, as the CO coverage increases, the distance between the adsorbed CO molecules gradually decreases, along with an increase in the interaction between the adsorbates. The number of configurations shows a trend of initially increasing and then decreasing (Table S4). Ultimately, nearly 7 million adsorption configurations are generated for the eight Cu surfaces (Table S5), representing an extremely large configuration space.

We propose a simple and efficient framework capable of rapidly and accurately predicting the CO adsorption energies of all stable configurations. The workflow is illustrated in Figure 1b, which depicts our comprehensive computational exploration of the configuration space. Initially, the entire configuration space is sampled randomly twice to obtain the first and second sampling spaces, respectively, with both sampling steps covering all surface coverage levels.

Subsequently, configurations from the more concise second sampling space undergo DFT structural optimization to obtain the CO adsorption energies of stable configurations, along with the trajectory of configuration optimization and the corresponding energies. Using these trajectories and energies as a dataset, a machine learning force field based on the DPMD deep potential architecture is trained, which effectively fits the interaction between adsorbates at different coverages.[56] The fitted force field is then used to optimize the structures of the larger first sampling space to obtain the CO adsorption energies of stable configurations. The resulting configuration-adsorption energy data can train a well-performing graph embedding network model, capable of accurately predicting the stable CO energies of approximately 7 million adsorption configurations in the target configuration space, despite using very simple feature combinations.

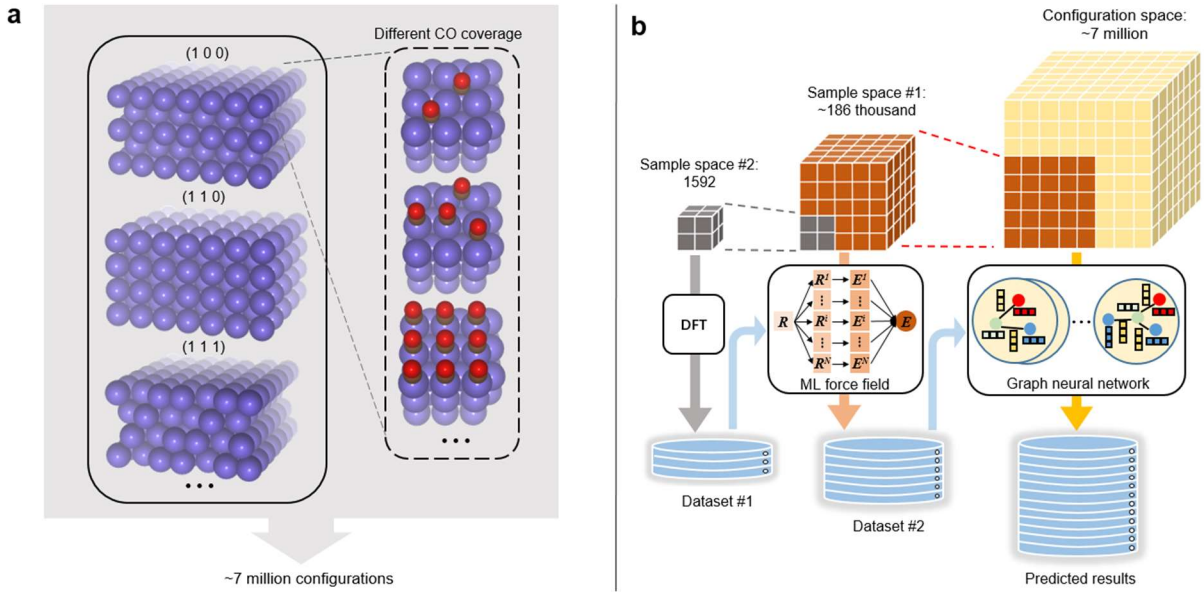

Figure1: Configuration Space and Workflow for CO Adsorption Energy Prediction on Cu Surfaces. **(a)** Schematic representation of CO adsorption configurations on Cu(100), Cu(110), and Cu(111) surfaces illustrating different CO coverages. The configurations exhibit varying distances between adsorbed CO molecules in relation to the coverage density, culminating in a broad spectrum of nearly 7 million configurations across eight Cu surfaces, as indicated by the expansive configuration space. **(b)** Depiction of the workflow: starting with a random selection of 186,000 potential configurations (Sample space 1), it narrows down to 1,592 configurations (Sample space 2) for DFT optimization. These optimized configurations train a DPMD-based ML force field, which is then used to predict adsorption energies for the initial sample space, allowing the graph embedding network to estimate stable-state energies for the extensive configuration space.

Compared to the total configurational space, the computational framework requires a significantly lower volume of initial data from DFT calculations, differing by three orders of magnitude, even though DFT calculations are generally considered to be highly resource-intensive. By introducing a machine-learned force field (MLFF) model with DFT accuracy, we have substantially enriched the training dataset for the adsorption energy prediction model. This approach cleverly circumvents the costly active learning process while enabling the

assessment and exploration of the complete, complex configurational space in a cost-measurable manner—a capability not present in previous studies.[5, 35-36, 45, 47] Moreover, this scalable framework for high-coverage configurational exploration can be flexibly defined and upgraded according to the user's needs.

Independent Adsorption Configuration Enumeration

To acquire the global stable structures of adsorption configurations, researchers typically enumerate and construct sets of configuration guesses that closely approximate local stable structures based on prior knowledge before DFT geometric optimization.[42-44, 48] These initial guesses often share similar or identical atomic bonding relationships with their corresponding local stable structures. After geometric optimization, the local stable structures with the lowest energy are usually considered the global stable structures of the adsorption configuration; in other words, the global stable structures are a subset of the collection of local stable structures. However, this manual enumeration method for guessing adsorption configurations is not suitable for the high-coverage adsorption configuration systems in our study, due to the richness and combinatory nature of adsorbable sites on the modeling surface.[42, 48] In this case, we must introduce an automated enumeration process for configuration guesses based on prior experience and conditional constraints. Since our research focuses on the impact of interactions between adsorbates on CO adsorption energy, the variability of adsorption sites is a key consideration in our enumeration of adsorption configuration guesses. Additionally, the global stable structures we focus on do not involve complex changes such as interface reconstruction or adsorbate desorption, at most only changes in the CO adsorption sites on the surface compared to the initial configuration guesses after geometric optimization, although studies have shown that high coverage of adsorbates can trigger surface reconstruction and significantly change the surface's catalytic properties.[34-36] For potential adsorbate desorption issues after geometric optimization, we can avoid them by introducing an empirical distance threshold in the initial guess modeling before optimization, effectively reducing the computational cost of unreasonable configuration guesses. In our studied systems, the differences in adsorption energy between adsorption configurations primarily depend on the adsorption sites, so enumerating the combination space of adsorption sites on the surface conveniently yields our target configuration guess space, which can be quickly achieved for a finite-sized slab.

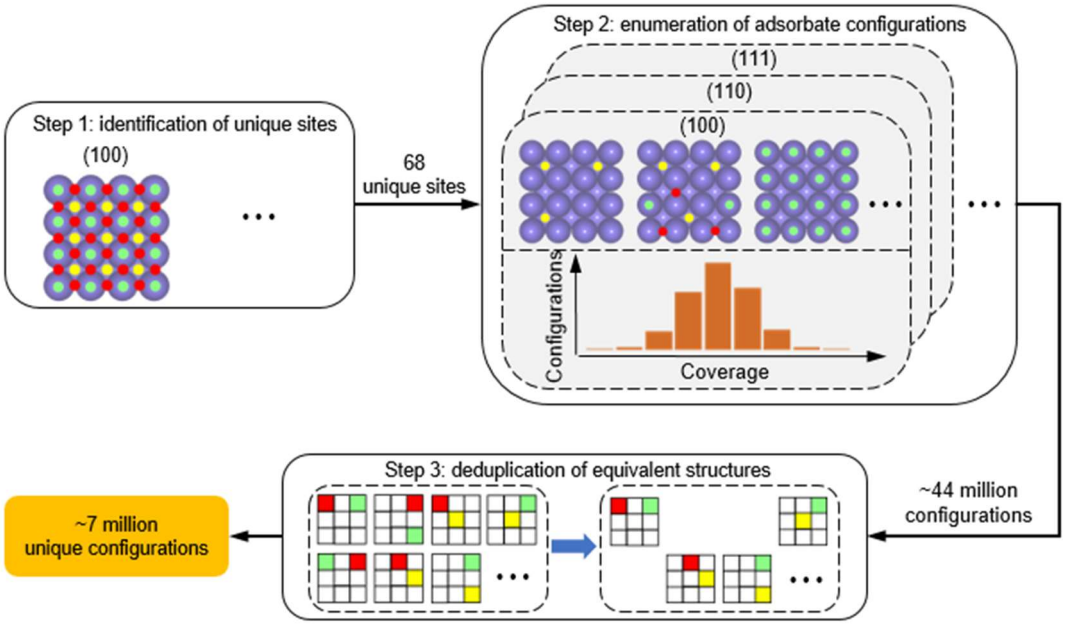

Figure 2: Enumeration of unique CO Adsorption Configurations. A three-step method for defining unique CO adsorption configurations on Cu surfaces. Initially, Step 1 identifies 68 distinct adsorption sites using graph theory to capture surface atom arrangements. Step 2 demonstrates the systematic filling of CO on these sites while adhering to spatial constraints, yielding approximately 44 million preliminary configurations. Step 3 applies symmetry operations to distill these down to around 7 million unique configurations, streamlining the dataset for further computational exploration.

The enumeration of adsorption configuration guess space is conducted on eight Cu surfaces, including (100), (110), (111), (210), (221), (310), (311), and (322), which are considered to be worth exploring by researchers.[57-61] As shown in Figure 2, the enumeration process is divided into three steps: surface site search, adsorption configuration enumeration, and deduplication of equivalent configuration guesses. In the site search part, we define the collection of Cu atoms on the surface that can bond with adsorbates and their surrounding environment as a site. Therefore, the types of sites depend on the size of the Cu atom collection and its local environment. Here, we abstract sites and their local environments into graphs using graph theory methods and determine the uniqueness of sites by judging whether the site graphs are isomorphic. Using graph theory methods, we conveniently identified 68 unique sites from the 8 Cu surfaces and used a combination letter naming method to distinguish different site types, for example, the "Bb" site type, where "B" indicates the site has a coordination number of n=2, and "b" indicates it is the second graph structure among sites with the same coordination number, and so on. This purely geometric definition of sites does not restrict the morphology of the sites, reducing the damage that biased understanding may cause to constructing a complete configuration guess space.[42-43] Its generality and scalability make it convenient to apply to the construction of configuration guesses in other high coverage systems.[21, 29, 62] The graph-theoretical site comparison method allows for a simple and rapid quantitative description of differences between sites.

After detecting all adsorption sites on the Cu surfaces, we used a method of filling CO molecules on the clean Cu surface with distance limitations to achieve the enumeration of

configuration guesses, with the main requirements being: CO adsorbs monodentately on the Cu surface with only C contacting Cu atoms; the orientation of CO molecules is set to the vector sum of the direction vector from its coordinating Cu atom to the C atom; the filling distance limitation requires that the interatomic distance between different CO molecules must not be less than 2.3 Å. Consequently, we obtained approximately 44 million initial adsorption configuration guesses, with the number of configurations enumerated on different index faces increasing with CO coverage before decreasing (Table S4). Based on the site type naming method, we named the adsorption configuration according to the combination types of sites they belong to, for example, "Aa2Ab1Da1Dc2" site combination type, indicating 2, 1, 1, 2 CO molecules adsorb on "Aa", "Ab", "Da", "Dc" types of sites, respectively. Moreover, we defined a simplified site combination type, such as the simplified type for "Aa2Ab1Da1Dc2" being "AD". Subsequent configuration data sampling calculations will be based on these two types of site combinations. Notably, the previous enumeration process did not consider the intrinsic symmetry of different Cu surfaces, for example, the Cu(111) surface corresponds to the p3m1 plane group (Table S8).[63-65] The existence of such planar symmetry results in a large number of duplicate structures in the enumerated configuration guesses. Through symmetry operations, we obtained approximately 7 million independent initial adsorption configuration guesses from the 44 million, significantly narrowing the target configuration space range. Compared to the graph-theoretical deduplication algorithm, this method not only has a crushing advantage in comparison speed but also can theoretically overcome the limitations of the graph isomorphism algorithm in comparing periodic crystal structures.[42] Overall, this enumeration process of the configuration space allows for a more comprehensive consideration of the adsorbate sequence space, thereby reducing the errors associated with energetics-based configuration sampling.[35, 42]

Machine Learning Force Field

Given the vast adsorption configuration space spanning across eight different Cu surfaces, it is imperative to leverage artificial intelligence to navigate this extensive configuration space. Two research approaches are considered viable: The first involves constructing machine learning force fields through the rich trajectory data obtained during the first-principles geometric optimization of a small set of adsorption configurations, followed by using the trained force field model to optimize the remaining adsorption configurations.[52] The second approach entails developing a deep learning model capable of directly predicting the steady-state adsorption energy from initial configuration guesses.[47, 49] Given that the construction of force fields can significantly utilize data from the structural optimization process, the initial DFT (Density Functional Theory) calculations required for the first strategy are considerably less. However, using the force field model to optimize the remaining configurations is also a time-consuming task, especially considering the configuration space volume closes seven million. Additionally, selecting a small number of representative configurations for DFT calculations from a vast and unevenly distributed sample space, particularly among high-index surface configurations, poses a challenging problem.

Therefore, after considering both the predictive accuracy of machine learning force fields and the prediction speed of deep learning models, we designed an integrated solution that uses

MLFF (Machine Learning Force Field) as a data augmenter for the adsorption energy prediction model. Initially, for low-index surfaces such as Cu(100), Cu(110), and Cu(111) depicted in Figure 1b, where the enumerated configuration count is low, we randomly select 20% of the unoptimized adsorption configurations for DFT calculations. For higher-index surfaces, we perform a primary sampling based on adsorption site combination types, followed by a secondary sampling based on simplified adsorption site combinations. The configurations obtained from secondary sampling undergo DFT structural optimization (S1.1). Subsequently, we train a force field model for the Cu-CO system with accuracy close to DFT calculations using the open-source and user-friendly deep learning architecture DPMD, which has been proven to have high simulation accuracy and efficiency in vast Si atomic systems.[56, 66] This force field model is then applied to optimize the remaining low-index surface configurations and those from the primary sampling. By expanding the training dataset with adsorption configurations using machine learning force fields, we can significantly address the issue of data scarcity faced when constructing deep learning models, thereby substantially improving model quality.[55]

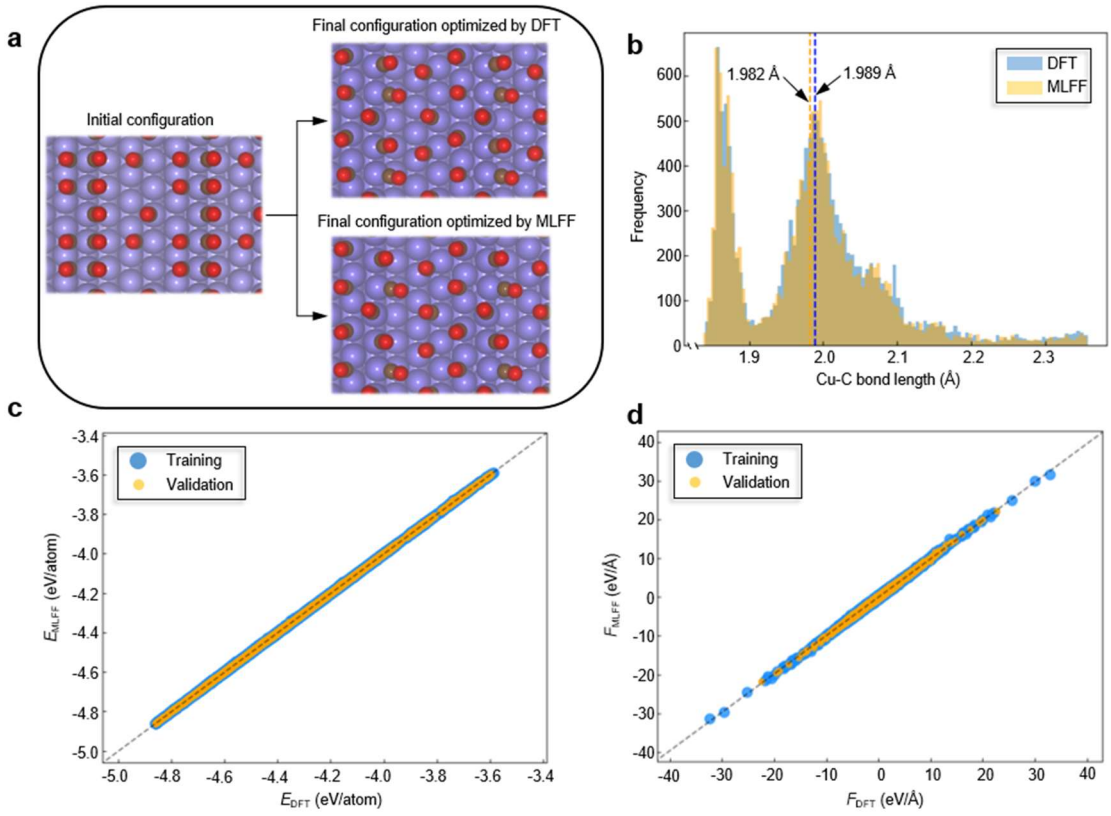

Figure 3: Evaluation of Machine Learning Force Field (MLFF) Accuracy. (a) Comparing the initial CO adsorption configuration with those optimized by DFT and MLFF, showing the MLFF's ability to replicate DFT-level structural accuracy on Cu surfaces. **(b)** Histogram of Cu-C bond lengths from stable-state configurations, highlighting the close match between MLFF and DFT results, with bond length discrepancies averaging less than 0.01 Å. **(c)** Scatter plot of the energy predictions, demonstrating the MLFF's high accuracy, with an RMSE for energy within 1 meV/atom, as validated against DFT calculations. **(d)** Corresponding force predictions plot, where the MLFF achieves an RMSE of less than 0.03 eV/Å, indicating the model's precision in capturing the forces in the Cu-CO system across a vast configuration space.

As shown in Figures 3c-d, our trained force field exhibits high accuracy, with RMSE (Root Mean Square Error) values for energy and force being <1 meV/atom and <0.03 eV/Å, respectively. The optimization of 1592 initial configuration guesses in the secondary sampling space using the well-fitted force field further assesses the force field quality: the steady-state adsorption configurations obtained from force field optimization almost perfectly match those obtained from DFT optimization (Figure 3a). Moreover, analyzing the distribution of Cu-C bond lengths in the steady-state adsorption configuration set reveals that the distribution from MLFF optimization closely aligns with that from DFT optimization (Figure 3b), with an average Cu-C bond length discrepancy of <0.01 Å. This demonstrates that the MLFF can achieve near-DFT calculation accuracy for adsorption configurations across eight Cu surfaces. The high-quality force field is attributed not only to the superior machine learning force field architecture but also to the effective sampling method—ensuring the sampled configuration guesses, i.e., the starting points for DFT geometric optimization, are as diverse as possible, facilitating a rich optimization trajectory that benefits model learning of more complex multi-body interactions.

Graph-Based Model for Adsorption Energy Prediction

In recent years, graph neural network models have shone brightly in material design and performance prediction, leveraging graph embeddings of materials for various predictive tasks.[67-70] One of their key advantages over other deep learning models lies in the natural suitability of graph structures for describing chemical and material structures, with nodes and edges representing atoms and their interactions, respectively. Hence, extracting high-quality graph data from materials is crucial. In our study, the interactions among CO molecules affect their adsorption energy on Cu surfaces, especially at high coverages. Previous research often overlooked non-bonding interactions beyond hydrogen bonds when constructing graph data, failing to accurately characterize adsorption structures.[47, 50] We propose an adsorption configuration graph data extraction method that effectively captures the impact of CO interactions on their adsorption energy, as shown in Figure 4a. The first step involves searching for atoms in contact with a CO molecule on the Cu surface, considering it as the central CO, within the van der Waals radius to form a neighbor atom set, including first-order neighbor COs in contact. The second step continues the search for atoms in contact with these first-order neighbor COs and builds local subgraphs for multiple neighbor sets centered on CO. The third step merges the central CO and its neighboring COs' local subgraphs into a feature graph representing the adsorption environment of the central CO. Different interaction types in the feature graph are assigned distinct indicator vectors during encoding, including non-bonding interactions between CO molecules, akin to the encoding of hydrogen bonds in previous research.[47, 50]

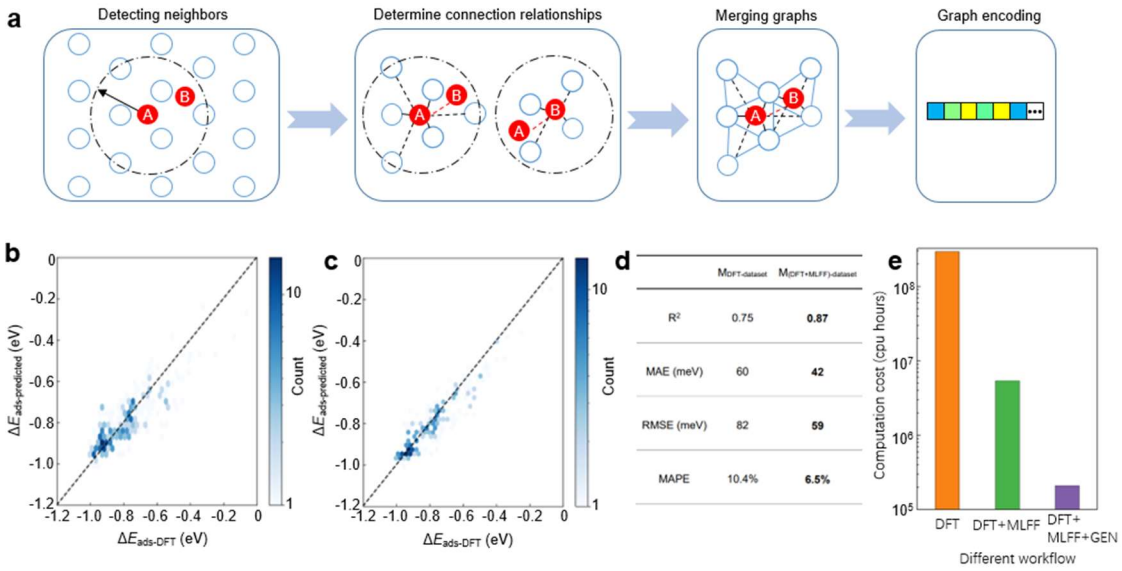

Figure 4: Graph Neural Network Model for CO Adsorption Prediction. (a) The graph data extraction method for CO adsorption configurations, detailing the steps from detecting neighboring atoms under van der Waals conditions to merging local subgraphs into a feature graph that accurately represents the adsorption environment of CO molecules on Cu surfaces. **(d)** The comparison of the GNN model's predictive performance between using only the DFT calculation dataset corresponding to **(b)** and using the DFT+MLFF calculation dataset corresponding to **(c)**. **(e)** The computational efficiency gains of the DFT+MLFF+GNN workflow compared to traditional DFT and DFT+MLFF methods, showcasing a significant reduction in computational cost and time, thus enabling the study of vast adsorption configuration spaces with enhanced efficiency.

Leveraging this graph feature extraction method, our trained graph neural network model demonstrated excellent predictive accuracy and generalization ability across eight index surfaces at varying coverages (Figure S2). The model's superior performance stems partly from more accurate graph descriptors. Unlike models that ignored CO non-bonding interactions when constructing graph data, our model significantly improved performance (Figure S3). Additionally, it benefited from the richness of training graph data, thanks to the expansion of training data via machine-learned force fields (MLFF), presenting an advantage over models trained solely on data from density functional theory (DFT) calculations. Using an expanded training set (about 186,000) under the same model architecture, our model outperformed the one trained only with DFT data (1,592), with a 16% increase in R^2 and a 28% reduction in RMSE (Figure 4d). Moreover, compared to direct DFT calculations or combined DFT+MLFF approaches for exploring target configuration spaces, our DFT+MLFF+GNN methodology significantly reduces computational costs by three and one orders of magnitude, respectively, greatly enhancing research efficiency in vast adsorption configuration spaces (Figure 4e). This acceleration allows for exploring extensive configuration spaces within a foreseeable short period, a capability previously unattainable.[35, 42, 44, 47] This dual-speed framework, integrating high-precision machine learning force fields with advanced graph representation learning, is also applicable to other catalytic systems with large search spaces, such as catalytic reaction path searches, stable adsorbate motif determination and protein-ligand structure prediction.[44, 71-72]

Coverage-Dependent Adsorption Energy on Different Indexed Surfaces

Leveraging our trained model for predicting adsorption energies, we calculated the steady-state CO adsorption energies for approximately 7 million configurations within the target configuration space, plotting CO adsorption energy versus coverage spectra for eight Cu crystallographic surfaces (Figure 5a). It was observed that each of the eight Cu surfaces corresponds to a unique CO coverage threshold, within which the adsorption energy of the most stable adsorption configurations changes minimally. Beyond this coverage threshold, the adsorption energy of the most stable configurations decreases significantly with increasing coverage. This trend aligns with physical intuition: at low coverages, the CO molecules in steady-state adsorption configurations are widely spaced, making non-bonding interactions between CO molecules negligible; however, at medium to high coverages, the surface arrangement of CO molecules in steady-state configurations becomes more compact, increasing molecular repulsion and thus increasing the system's potential energy, leading to decreased adsorption energies for CO molecules. Furthermore, aside from the (100) and (111) surfaces (where all surface atoms have the same coordination number), CO molecules preferentially occupy lower-coordination Cu sites that are energetically less favorable, and with increasing coverage, gradually cover higher-coordination Cu sites (Figure S4). At the same time, the average coordination number of Cu atoms occupied by CO at each coverage level remains lower than the average coordination number of surface Cu atoms, indicating a clear lowest-energy orientation for CO adsorption. These computational results are consistent with previous research findings.[40-41, 73] Understanding the ease of C-C coupling on different Cu surfaces is crucial for developing Cu-based nanometal catalysts with high selectivity for C_{2+} products in CO_2RR reactions, as easier C-C coupling between CO molecules leads to higher selectivity for C_{2+} products. [16, 18-20, 74]

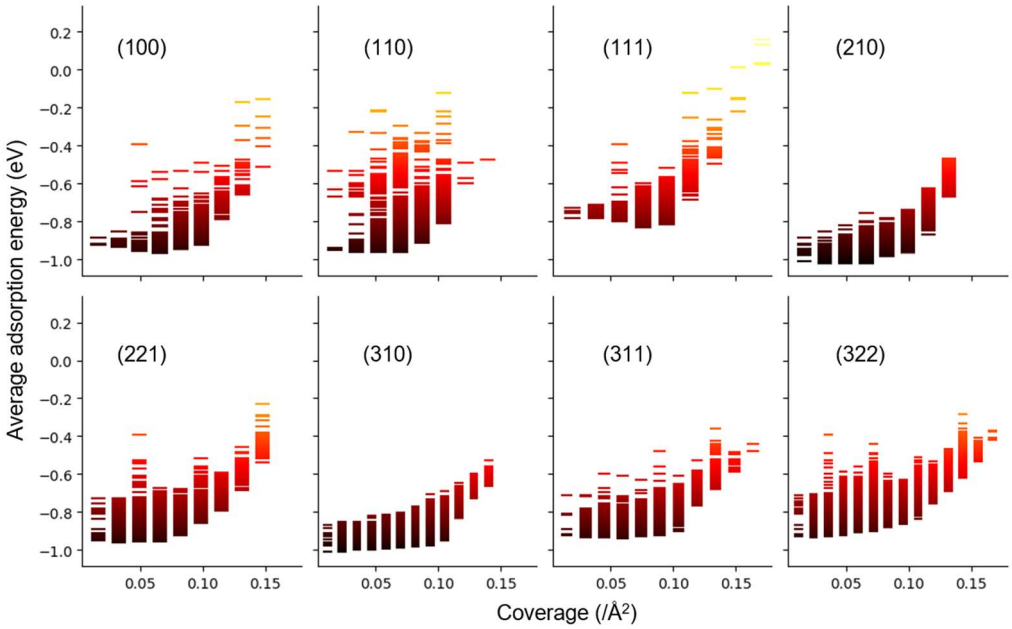

Figure 5: Coverage-Dependent CO Adsorption Energies on Cu Surfaces. The vertical axis corresponds to the average adsorption energy of CO, while the horizontal axis represents the number of CO molecules per unit area. The darker the bar color, the greater the average adsorption energy of CO.

Here, we employed two straightforward metrics to evaluate the ease of C-C coupling on Cu surfaces. The first metric is the Mean Minimum C-C Distance (MMCD) within the set of most stable adsorption configurations at various coverages (see S4.1), which serves as an indicator of the probability of C-C coupling. A smaller MMCD suggests a higher likelihood of coupling. The second metric is the characteristic coverage of the surface: taking the densely packed (111) surface as a reference and using its maximum adsorption energy as a threshold, the maximum coverage achievable by other surfaces without falling below this adsorption energy threshold is deemed their characteristic coverage. To facilitate successful C-C coupling, CO must exhibit sufficient adsorption strength on Cu surfaces to prevent the reactants from desorbing, which would interrupt the coupling reaction. Moreover, compared to the MMCD, the surface's characteristic coverage offers a more macroscopic dimension for representing the probability of C-C coupling, providing a holistic view. As illustrated in Figure 5b, we analyzed these two metrics across eight Cu surfaces and found that the (310) surface exhibits the best C-C coupling performance, while the (111) surface performs the worst. The performance ranking of (310) > (210) > (311) > (100) > (111) is largely in agreement with experimental observations.[59, 73] High-index surfaces tend to have smaller MMCDs and greater characteristic coverages, indicating a higher probability of C-C coupling and better selectivity for C_{2+} products. This finding aligns with our current theoretical and experimental research, which shows that high-index surfaces offer a richer variety of surface sites and an abundance of low-coordination surface Cu atoms. These features provide more stable adsorption sites and a superior surface electronic environment conducive to C-C coupling.[75-77] Additionally, the (322) surface emerged as a potential candidate due to its MMCD and characteristic coverage closely approaching those of the (310) surface, which has been experimentally proven to exhibit excellent selectivity for C_{2+} products.[59]

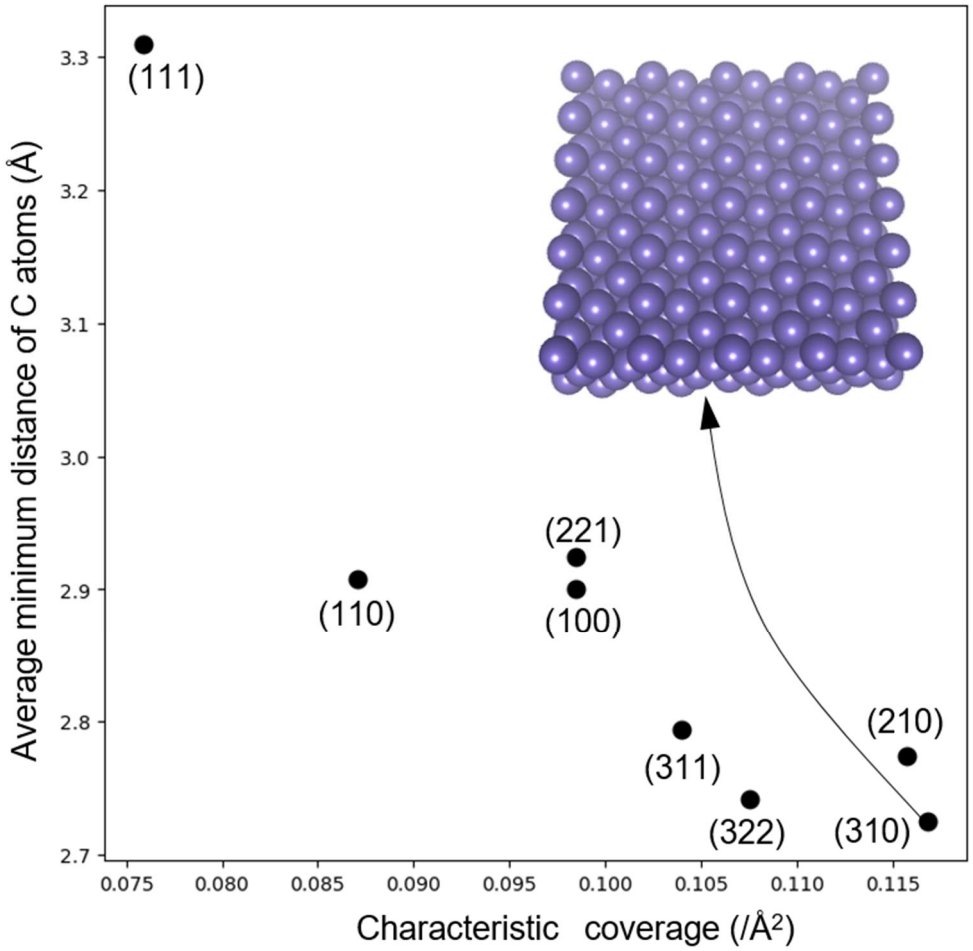

Figure 6: Correlation between C-C Distance and Coverage for Cu-Catalyzed Coupling. Surfaces like Cu(310) with smaller C-C distances and higher characteristic coverages are identified as optimal for C-C coupling, enhancing selectivity for C_{2+} products in CO_2 reduction reactions. The inset illustrates the surface model of Cu(310).

Conclusions

In conclusion, our investigation into the adsorption configurations of CO on Cu surfaces unveils critical insights into the mechanisms underlying electrocatalytic reactions. By leveraging advanced computational techniques, we have mapped out the energy landscapes of nearly 7 million configurations, identifying key trends in CO adsorption energies across different surface indices and coverages. Our findings underscore the importance of surface coverage in dictating the stability and activity of adsorption configurations, with implications for the efficiency of CO_2RR processes. The development and application of a machine learning force field, complemented by a graph-based adsorption energy prediction model, have significantly enhanced our ability to predict and understand the complex interactions at play. The discernment of high-index Cu surfaces as favorable for C-C coupling not only aligns with experimental observations but also opens new avenues for the design of catalysts with heightened selectivity for C_{2+} product formation. This work not only advances our theoretical understanding of catalytic mechanisms at high coverage but also sets the stage for future

research aimed at optimizing catalyst designs for sustainable energy conversion technologies.

Reference

1. Beck, Arik; Paunović, Vladimir; van Bokhoven, Jeroen A., Identifying and avoiding dead ends in the characterization of heterogeneous catalysts at the gas–solid interface. *Nature Catalysis* 2023, 6, 873-884.
2. Li, Xinzhe; Mitchell, Sharon; Fang, Yiyun; Li, Jun; Perez-Ramirez, Javier; Lu, Jiong, Advances in heterogeneous single-cluster catalysis. *Nature Reviews Chemistry* 2023, 7, 754-767.
3. Bruix, Albert; Margraf, Johannes T.; Andersen, Mie; Reuter, Karsten, First-principles-based multiscale modelling of heterogeneous catalysis. *Nature Catalysis* 2019, 2, 659-670.
4. Handoko, Albertus D.; Wei, Fengxia; Jenndy; Yeo, Boon Siang; Seh, Zhi Wei, Understanding heterogeneous electrocatalytic carbon dioxide reduction through operando techniques. *Nat. Catal.* 2018, 1, 922-934.
5. Tran, Kevin; Ulissi, Zachary W., Active learning across intermetallics to guide discovery of electrocatalysts for CO_2 reduction and H_2 evolution. *Nat. Catal.* 2018, 1, 696-703.
6. Greeley, J.; Stephens, I. E. L.; Bondarenko, A. S.; Johansson, T. P.; Hansen, H. A.; Jaramillo, T. F.; Rossmeisl, J.; Chorkendorff, I.; Nørskov, J. K., Alloys of platinum and early transition metals as oxygen reduction electrocatalysts. *Nature Chemistry* 2009, 1, 552-556.
7. Wu, Zhichao; Li, Zhe; Li, Yongxiu; Zhang, Yuhua; Li, Jinlin, Improving the DFT computational accuracy for CO activation on Fe surfaces by Bayesian error estimation functional with van der Waals correlation. *Computational and Theoretical Chemistry* 2023, 1219, 113968.
8. Araujo, Rafael B.; Rodrigues, Gabriel L. S.; dos Santos, Egon Campos; Pettersson, Lars G. M., Adsorption energies on transition metal surfaces: towards an accurate and balanced description. *Nature Communications* 2022, 13, 6853.
9. Nørskov, J. K.; Bligaard, T.; Logadottir, A.; Kitchin, J. R.; Chen, J. G.; Pandelov, S.; Stimming, U., Trends in the Exchange Current for Hydrogen Evolution. *Journal of The Electrochemical Society* 2005, 152, J23.
10. Nørskov, J. K.; Rossmeisl, J.; Logadottir, A.; Lindqvist, L.; Kitchin, J. R.; Bligaard, T.; Jónsson, H., Origin of the Overpotential for Oxygen Reduction at a Fuel-Cell Cathode. *J. Phys. Chem. B* 2004, 108, 17886-17892.
11. Greeley, Jeff; Jaramillo, Thomas F.; Bonde, Jacob; Chorkendorff, Ib; Nørskov, Jens K., Computational high-throughput screening of electrocatalytic materials for hydrogen evolution. *Nature Materials* 2006, 5, 909-913.
12. Liu, Xinyan; Xiao, Jianping; Peng, Hongjie; Hong, Xin; Chan, Karen; Nørskov, Jens K., Understanding trends in electrochemical carbon dioxide reduction rates. *Nature Communications* 2017, 8, 15438.
13. Li, Jun; Wang, Ziyun; McCallum, Christopher; Xu, Yi; Li, Fengwang; Wang, Yuhang; Gabardo, Christine M.; Dinh, Cao-Thang; Zhuang, Tao-Tao; Wang, Liang; Howe, Jane Y.; Ren, Yang; Sargent, Edward H.; Sinton, David, Constraining CO coverage on copper promotes high-efficiency ethylene electroproduction. *Nature Catalysis* 2019, 2, 1124-1131.
14. Chen, Yangshen; Lyu, Naixin; Zhang, Junbo; Yan, Shuai; Peng, Chen; Yang, Chao; Lv,

Ximeng; Hu, Cejun; Kuang, Min; Zheng, Gengfeng, Tailoring the *CO and *H Coverage for Selective CO_2 Electroreduction to CH4 or C2H4. *Small* 2023, n/a, 2308004.
15. Zhang, Tingting; Yuan, Bowen; Wang, Wenlong; He, Jing; Xiang, Xu, Tailoring *H Intermediate Coverage on the CuAl2O4/CuO Catalyst for Enhanced Electrocatalytic CO_2 Reduction to Ethanol. *Angewandte Chemie International Edition* 2023, 62, e202302096.
16. Jin, Jian; Wicks, Joshua; Min, Qiuhong; Li, Jun; Hu, Yongfeng; Ma, Jingyuan; Wang, Yu; Jiang, Zheng; Xu, Yi; Lu, Ruihu; Si, Gangzheng; Papangelakis, Panagiotis; Shakouri, Mohsen; Xiao, Qunfeng; Ou, Pengfei; Wang, Xue; Chen, Zhu; Zhang, Wei; Yu, Kesong; Song, Jiayang; Jiang, Xiaohang; Qiu, Peng; Lou, Yuanhao; Wu, Dan; Mao, Yu; Ozden, Adnan; Wang, Chundong; Xia, Bao Yu; Hu, Xiaobing; Dravid, Vinayak P.; Yiu, Yun-Mui; Sham, Tsun-Kong; Wang, Ziyun; Sinton, David; Mai, Liqiang; Sargent, Edward H.; Pang, Yuanjie, Constrained C2 adsorbate orientation enables CO-to-acetate electroreduction. *Nature* 2023, 617, 724-729.
17. Dorakhan, Roham; Grigioni, Ivan; Lee, Byoung-Hoon; Ou, Pengfei; Abed, Jehad; O'Brien, Colin; Sedighian Rasouli, Armin; Plodinec, Milivoj; Miao, Rui Kai; Shirzadi, Erfan; Wicks, Joshua; Park, Sungjin; Lee, Geonhui; Zhang, Jinqiang; Sinton, David; Sargent, Edward H., A silver–copper oxide catalyst for acetate electrosynthesis from carbon monoxide. *Nature Synthesis* 2023, 2, 448-457.
18. Hou, Jiajie; Chang, Xiaoxia; Li, Jing; Xu, Bingjun; Lu, Qi, Correlating CO Coverage and CO Electroreduction on Cu via High-Pressure in Situ Spectroscopic and Reactivity Investigations. *Journal of the American Chemical Society* 2022, 144, 22202-22211.
19. Zheng, Yiqun; Zhang, Jiawei; Ma, Zesong; Zhang, Gongguo; Zhang, Haifeng; Fu, Xiaowei; Ma, Yanyun; Liu, Feng; Liu, Maochang; Huang, Hongwen, Seeded Growth of Gold–Copper Janus Nanostructures as a Tandem Catalyst for Efficient Electroreduction of CO_2 to C_{2+} Products. *Small* 2022, 18, 2201695.
20. Sun, Weipei; Wang, Peng; Jiang, Yawen; Jiang, Zhiwei; Long, Ran; Chen, Zheng; Song, Pin; Sheng, Tian; Wu, Zhengcui; Xiong, Yujie, V-Doped Cu2Se Hierarchical Nanotubes Enabling Flow-Cell CO_2 Electroreduction to Ethanol with High Efficiency and Selectivity. *Advanced Materials* 2022, 34, 2207691.
21. Deshpande, Siddharth; Greeley, Jeffrey, First-Principles Analysis of Coverage, Ensemble, and Solvation Effects on Selectivity Trends in NO Electroreduction on Pt3Sn Alloys. *ACS Catalysis* 2020, 10, 9320-9327.
22. Katsounaros, Ioannis; Figueiredo, Marta C.; Chen, Xiaoting; Calle-Vallejo, Federico; Koper, Marc T. M., Structure- and Coverage-Sensitive Mechanism of NO Reduction on Platinum Electrodes. *ACS Catalysis* 2017, 7, 4660-4667.
23. Ko, Byung Hee; Hasa, Bjorn; Shin, Haeun; Zhao, Yaran; Jiao, Feng, Electrochemical Reduction of Gaseous Nitrogen Oxides on Transition Metals at Ambient Conditions. *Journal of the American Chemical Society* 2022, 144, 1258-1266.
24. Tan, Zhe; Haneda, Masaaki; Kitagawa, Hiroshi; Huang, Bo, Slow Synthesis Methodology-Directed Immiscible Octahedral PdxRh1−x Dual-Atom-Site Catalysts for Superior Three-Way Catalytic Activities over Rh. *Angewandte Chemie International Edition* 2022, 61, e202202588.
25. Muravev, Valery; Spezzati, Giulia; Su, Ya-Qiong; Parastaev, Alexander; Chiang, Fu-Kuo; Longo, Alessandro; Escudero, Carlos; Kosinov, Nikolay; Hensen, Emiel J. M., Interface dynamics of Pd–CeO2 single-atom catalysts during CO oxidation. *Nature Catalysis* 2021, 4, 469-478.

26. Abdel-Mageed, Ali M.; Rungtaweevoranit, Bunyarat; Impeng, Sarawoot; Bansmann, Joachim; Rabeah, Jabor; Chen, Shilong; Häring, Thomas; Namuangrak, Supawadee; Faungnawakij, Kajornsak; Brückner, Angelika; Behm, R. Jürgen, Unveiling the CO Oxidation Mechanism over a Molecularly Defined Copper Single-Atom Catalyst Supported on a Metal–Organic Framework. *Angewandte Chemie International Edition* 2023, 62, e202301920.
27. van Spronsen, Matthijs A.; Frenken, Joost W. M.; Groot, Irene M. N., Surface science under reaction conditions: CO oxidation on Pt and Pd model catalysts. *Chem Soc Rev* 2017, 46, 4347-4374.
28. Weststrate, C. J.; Sharma, Devyani; Garcia Rodriguez, Daniel; Gleeson, Michael A.; Fredriksson, Hans O. A.; Niemantsverdriet, J. W., Mechanistic insight into carbon-carbon bond formation on cobalt under simulated Fischer-Tropsch synthesis conditions. *Nature Communications* 2020, 11, 750.
29. Ojeda, Manuel; Nabar, Rahul; Nilekar, Anand U.; Ishikawa, Akio; Mavrikakis, Manos; Iglesia, Enrique, CO activation pathways and the mechanism of Fischer–Tropsch synthesis. *Journal of Catalysis* 2010, 272, 287-297.
30. Rommens, Konstantijn Tom; Saeys, Mark, Molecular Views on Fischer–Tropsch Synthesis. *Chemical Reviews* 2023, 123, 5798-5858.
31. Zhang, Minhua; Ren, Jie; Yu, Yingzhe, Insights into the Hydrogen Coverage Effect and the Mechanism of Fischer–Tropsch to Olefins Process on Fe5C2 (510). *ACS Catalysis* 2020, 10, 689-701.
32. Yao, Zihao; Guo, Chenxi; Mao, Yu; Hu, P., Quantitative Determination of C–C Coupling Mechanisms and Detailed Analyses on the Activity and Selectivity for Fischer–Tropsch Synthesis on Co(0001): Microkinetic Modeling with Coverage Effects. *ACS Catalysis* 2019, 9, 5957-5973.
33. Zhuo, Mingkun; Borgna, Armando; Saeys, Mark, Effect of the CO coverage on the Fischer–Tropsch synthesis mechanism on cobalt catalysts. *Journal of Catalysis* 2013, 297, 217-226.
34. Eren, Baran; Zherebetskyy, Danylo; Patera, Laerte L.; Wu, Cheng Hao; Bluhm, Hendrik; Africh, Cristina; Wang, Lin-Wang; Somorjai, Gabor A.; Salmeron, Miquel, Activation of Cu(111) surface by decomposition into nanoclusters driven by CO adsorption. *Science* 2016, 351, 475-478.
35. Sumaria, Vaidish; Sautet, Philippe, CO organization at ambient pressure on stepped Pt surfaces: first principles modeling accelerated by neural networks. *Chemical Science* 2021, 12, 15543-15555.
36. Sumaria, Vaidish; Nguyen, Luan; Tao, Franklin Feng; Sautet, Philippe, Atomic-Scale Mechanism of Platinum Catalyst Restructuring under a Pressure of Reactant Gas. *Journal of the American Chemical Society* 2023, 145, 392-401.
37. Pineda, M.; Stamatakis, M., Beyond mean-field approximations for accurate and computationally efficient models of on-lattice chemical kinetics. *The Journal of Chemical Physics* 2017, 147, 024105.
38. Schmidt, David J.; Chen, Wei; Wolverton, C.; Schneider, William F., Performance of Cluster Expansions of Coverage-Dependent Adsorption of Atomic Oxygen on Pt(111). *J Chem Theory Comput* 2012, 8, 264-273.
39. Wu, C.; Schmidt, D. J.; Wolverton, C.; Schneider, W. F., Accurate coverage-dependence

incorporated into first-principles kinetic models: Catalytic NO oxidation on Pt (111). *Journal of Catalysis* 2012, 286, 88-94.
40. Grabow, Lars C.; Hvolbæk, Britt; Nørskov, Jens K., Understanding Trends in Catalytic Activity: The Effect of Adsorbate–Adsorbate Interactions for CO Oxidation Over Transition Metals. *Topics in Catalysis* 2010, 53, 298-310.
41. Lausche, Adam C.; Medford, Andrew J.; Khan, Tuhin Suvra; Xu, Yue; Bligaard, Thomas; Abild-Pedersen, Frank; Nørskov, Jens K.; Studt, Felix, On the effect of coverage-dependent adsorbate–adsorbate interactions for CO methanation on transition metal surfaces. *Journal of Catalysis* 2013, 307, 275-282.
42. Deshpande, Siddharth; Maxson, Tristan; Greeley, Jeffrey, Graph theory approach to determine configurations of multidentate and high coverage adsorbates for heterogeneous catalysis. *npj Comput. Mater.* 2020, 6.
43. Boes, Jacob R.; Mamun, Osman; Winther, Kirsten; Bligaard, Thomas, Graph Theory Approach to High-Throughput Surface Adsorption Structure Generation. *JOURNAL OF PHYSICAL CHEMISTRY A* 2019, 123, 2281-2285.
44. Gu, Geun Ho; Lee, Miriam; Jung, Yousung; Vlachos, Dionisios G., Automated exploitation of the big configuration space of large adsorbates on transition metals reveals chemistry feasibility. *Nature Communications* 2022, 13, 2087.
45. Ulissi, Zachary W.; Tang, Michael T.; Xiao, Jianping; Liu, Xinyan; Torelli, Daniel A.; Karamad, Mohammadreza; Cummins, Kyle; Hahn, Christopher; Lewis, Nathan S.; Jaramillo, Thomas F.; Chan, Karen; Nørskov, Jens K., Machine-Learning Methods Enable Exhaustive Searches for Active Bimetallic Facets and Reveal Active Site Motifs for CO_2 Reduction. *ACS Catalysis* 2017, 7, 6600-6608.
46. Lu, Zhuole; Chen, Zhi Wen; Singh, Chandra Veer, Neural Network-Assisted Development of High-Entropy Alloy Catalysts: Decoupling Ligand and Coordination Effects. *Matter* 2020, 3, 1318-1333.
47. Ghanekar, P. G.; Deshpande, S.; Greeley, J., Adsorbate chemical environment-based machine learning framework for heterogeneous catalysis. *Nat Commun* 2022, 13, 5788.
48. Xu, Wenbin; Reuter, Karsten; Andersen, Mie, Predicting binding motifs of complex adsorbates using machine learning with a physics-inspired graph representation. *Nature Computational Science* 2022, 2, 443-450.
49. Chanussot, Lowik; Das, Abhishek; Goyal, Siddharth; Lavril, Thibaut; Shuaibi, Muhammed; Riviere, Morgane; Tran, Kevin; Heras-Domingo, Javier; Ho, Caleb; Hu, Weihua; Palizhati, Aini; Sriram, Anuroop; Wood, Brandon; Yoon, Junwoong; Parikh, Devi; Zitnick, C. Lawrence; Ulissi, Zachary, Open Catalyst 2020 (OC20) Dataset and Community Challenges. *ACS Catalysis* 2021, 11, 6059-6072.
50. Bang, Kihoon; Hong, Doosun; Park, Youngtae; Kim, Donghun; Han, Sang Soo; Lee, Hyuck Mo, Machine learning-enabled exploration of the electrochemical stability of real-scale metallic nanoparticles. *Nature Communications* 2023, 14, 3004.
51. Pablo-García, Sergio; Morandi, Santiago; Vargas-Hernández, Rodrigo A.; Jorner, Kjell; Ivković, Žarko; López, Núria; Aspuru-Guzik, Alán, Fast evaluation of the adsorption energy of organic molecules on metals via graph neural networks. *Nature Computational Science* 2023, 3, 433-442.
52. Yang, Y.; Jimenez-Negron, O. A.; Kitchin, J. R., Machine-learning accelerated geometry

optimization in molecular simulation. *J Chem Phys* 2021, 154, 234704.
53. Foggia, Pasquale; Sansone, Carlo; Vento, Mario, A Performance Comparison of Five Algorithms for Graph Isomorphism. *3rd IAPR TC-15 Workshop on Graph-based Representations in Pattern Recognition* 2001.
54. Jenner, Birgit; Köbler, Johannes; McKenzie, Pierre; Torán, Jacobo, Completeness results for graph isomorphism. *Journal of Computer and System Sciences* 2003, 66, 549-566.
55. Jha, Dipendra; Gupta, Vishu; Ward, Logan; Yang, Zijiang; Wolverton, Christopher; Foster, Ian; Liao, Wei-keng; Choudhary, Alok; Agrawal, Ankit, Enabling deeper learning on big data for materials informatics applications. *Scientific Reports* 2021, 11, 4244.
56. Zhang, L.; Han, J.; Wang, H.; Car, R.; E, W., Deep Potential Molecular Dynamics: A Scalable Model with the Accuracy of Quantum Mechanics. *Phys Rev Lett* 2018, 120, 143001.
57. Pérez-Gallent, Elena; Figueiredo, Marta C.; Calle-Vallejo, Federico; Koper, Marc T. M., Spectroscopic Observation of a Hydrogenated CO Dimer Intermediate During CO Reduction on Cu(100) Electrodes. *Angewandte Chemie International Edition* 2017, 56, 3621-3624.
58. Nakano, Haruhisa; Nakamura, Isao; Fujitani, Tadahiro; Nakamura, Junji, Structure-Dependent Kinetics for Synthesis and Decomposition of Formate Species over Cu(111) and Cu(110) Model Catalysts. *The Journal of Physical Chemistry B* 2001, 105, 1355-1365.
59. Hori, Y.; Takahashi, I.; Koga, O.; Hoshi, N., Electrochemical reduction of carbon dioxide at various series of copper single crystal electrodes. *Journal of Molecular Catalysis A: Chemical* 2003, 199, 39-47.
60. Wang, Sha-sha; Jian, Min-zhen; Su, Hai-Yan; Li, Wei-Xue, First-Principles microkinetic study of methanol synthesis on Cu(221) and ZnCu(221) surfaces. *Chinese Journal of Chemical Physics* 2018, 31, 284-290.
61. Schouten, Klaas Jan P.; Pérez Gallent, Elena; Koper, Marc T. M., Structure Sensitivity of the Electrochemical Reduction of Carbon Monoxide on Copper Single Crystals. *ACS Catalysis* 2013, 3, 1292-1295.
62. Guo, Wei; Vlachos, Dionisios G., Effect of local metal microstructure on adsorption on bimetallic surfaces: Atomic nitrogen on Ni/Pt(111). *The Journal of Chemical Physics* 2013, 138, 174702.
63. Stróż, K., Plane groups - From basic to advanced crystallographic concepts. *Zeitschrift Fur Kristallographie - Z KRISTALLOGR* 2003, 218, 642-649.
64. Hoffmann, Frank, Symmetry in the Plane: About Wallpaper Patterns, Islamic Mosaics, Drawings from Escher, and Heterogeneous Catalysts. In *Introduction to Crystallography*, Hoffmann, F., Ed. Springer International Publishing: Cham, 2020; pp 127-150.
65. Hahn, Th, The 17 plane groups (two-dimensional space groups). In *International Tables for Crystallography Volume A: Space-group symmetry*, Hahn, T., Ed. Springer Netherlands: Dordrecht, 2002; pp 92-109.
66. Lu, Denghui; Wang, Han; Chen, Mohan; Lin, Lin; Car, Roberto; E, Weinan; Jia, Weile; Zhang, Linfeng, 86 PFLOPS Deep Potential Molecular Dynamics simulation of 100 million atoms with ab initio accuracy. *Computer Physics Communications* 2021, 259, 107624.
67. Weng, Mouyi; Wang, Zhi; Qian, Guoyu; Ye, Yaokun; Chen, Zhefeng; Chen, Xin; Zheng, Shisheng; Pan, Feng, Identify crystal structures by a new paradigm based on graph theory for building materials big data. *Sci. China-Chem.* 2019, 62, 982-986.
68. Li, Shunning; Chen, Zhefeng; Wang, Zhi; Weng, Mouyi; Li, Jianyuan; Zhang, Mingzheng; Lu, Jing; Xu, Kang; Pan, Feng, Graph-based discovery and analysis of atomic-scale one-

dimensional materials. *National Science Review* 2022, 9, nwac028.
69. Li, Shunning; Liu, Yuanji; Chen, Dong; Jiang, Yi; Nie, Zhiwei; Pan, Feng, Encoding the atomic structure for machine learning in materials science. *WIREs Computational Molecular Science* 2021, 12.
70. Xie, Tian; Grossman, Jeffrey C., Crystal Graph Convolutional Neural Networks for an Accurate and Interpretable Prediction of Material Properties. *Physical Review Letters* 2018, 120, 145301.
71. Steiner, Miguel; Reiher, Markus, Autonomous Reaction Network Exploration in Homogeneous and Heterogeneous Catalysis. *Topics in Catalysis* 2022, 65, 6-39.
72. Qiao, Zhuoran; Nie, Weili; Vahdat, Arash; Miller, Thomas F.; Anandkumar, Animashree, State-specific protein–ligand complex structure prediction with a multiscale deep generative model. *Nature Machine Intelligence* 2024, 6, 195-208.
73. Huang, Yun; Handoko, Albertus D.; Hirunsit, Pussana; Yeo, Boon Siang, Electrochemical Reduction of CO_2 Using Copper Single-Crystal Surfaces: Effects of CO* Coverage on the Selective Formation of Ethylene. *ACS Catalysis* 2017, 7, 1749-1756.
74. Yan, Xupeng; Chen, Chunjun; Wu, Yahui; Chen, Yizhen; Zhang, Jianling; Feng, Rongjuan; Zhang, Jing; Han, Buxing, Boosting CO_2 electroreduction to C_{2+} products on fluorine-doped copper. *Green Chemistry* 2022, 24, 1989-1994.
75. Fang, Wensheng; Lu, Ruihu; Li, Fu-Min; Wu, Dan; Yue, Kaihang; He, Chaohui; Mao, Yu; Guo, Wei; You, Bo; Song, Fei; Yao, Tao; Wang, Ziyun; Xia, Bao Yu, Low-coordination Nanocrystalline Copper-based Catalysts through Theory-guided Electrochemical Restructuring for Selective CO_2 Reduction to Ethylene. *Angewandte Chemie International Edition* 2024, n/a, e202319936.
76. Wang, Yuxuan; Li, Boyang; Xue, Bin; Libretto, Nicole; Xie, Zhenhua; Shen, Hao; Wang, Canhui; Raciti, David; Marinkovic, Nebojsa; Zong, Han; Xie, Wenjun; Li, Ziyuan; Zhou, Guangye; Vitek, Jeff; Chen, Jingguang G.; Miller, Jeffery; Wang, Guofeng; Wang, Chao, CO electroreduction on single-atom copper. *Science Advances* 9, eade3557.
77. Reller, Christian; Krause, Ralf; Volkova, Elena; Schmid, Bernhard; Neubauer, Sebastian; Rucki, Andreas; Schuster, Manfred; Schmid, Günter, Selective Electroreduction of CO_2 toward Ethylene on Nano Dendritic Copper Catalysts at High Current Density. *Advanced Energy Materials* 2017, 7, 1602114.